HHS Public Access

Author manuscript

Cell Rep. Author manuscript; available in PMC 2017 October 30.

Published in final edited form as:

Cell Rep. 2017 October 24; 21(4): 979–993. doi:10.1016/j.celrep.2017.09.084.

The Conserved ATM Kinase RAG2-S365 Phosphorylation Site Limits Cleavage Events in Individual Cells Independent of Any Repair Defect

Susannah L. Hewitt[1], **Jason B. Wong**[1], **Ji-Hoon Lee**[2], **Mayilaadumveettil Nishana**[1], **Hongxi Chen**[1], **Marc Coussens**[1,3], **Suzzette M. Arnal**[1,4], **Lili M. Blumenberg**[1], **David B. Roth**[3], **Tanya T. Paull**[2], and **Jane A. Skok**[1,5,*]

[1]Department of Pathology, New York University School of Medicine, New York, NY 10016, USA

[2]Howard Hughes Medical Institute, Department of Molecular Biosciences, Institute for Cellular and Molecular Biology, University of Texas at Austin, Austin, TX 78712, USA

[3]Department of Pathology and Laboratory Medicine, Perelman School of Medicine, University of Pennsylvania, Philadelphia, PA 19104, USA

SUMMARY

Many DNA lesions associated with lymphoid malignancies are linked to off-target cleavage by the RAG1/2 recombinase. However, off-target cleavage has mostly been analyzed in the context of DNA repair defects, confounding any mechanistic understanding of cleavage deregulation. We identified a conserved SQ phosphorylation site on RAG2 365 to 366 that is involved in feedback control of RAG cleavage. Mutation of serine 365 to a non-phosphorylatable alanine permits bi-allelic and bi-locus RAG-mediated breaks in the same cell, leading to reciprocal translocations. This phenomenon is analogous to the phenotype we described for ATM kinase inactivation. Here, we establish deregulated cleavage itself as a driver of chromosomal instability without the associated repair defect. Intriguingly, a RAG2-S365E phosphomimetic rescues the deregulated cleavage of ATM inactivation, reducing the incidence of reciprocal translocations. These data support a model in which feedback control of cleavage and maintenance of genome stability involves ATM-mediated phosphorylation of RAG2.

In Brief

*Correspondence: jane.skok@nyumc.org.

[4]Present address: Biological Sciences Department, Columbia University, New York, NY 10027, USA

[5]Lead Contact

SUPPLEMENTAL INFORMATION

Supplemental Information includes Supplemental Experimental Procedures, four figures, and seven tables and can be found with this article online at https://doi.org/10.1016/j.celrep.2017.09.084.

AUTHOR CONTRIBUTIONS

S.L.H. designed and carried out the experiments in Figures 1, 2, 3, 4, 5, 6, and 7. J.B.W. and S.L.H. carried out the experiments in Figure 5. M.C. designed and carried out the experiments in Figures 3F and 3G. S.M.A. designed and carried out the experiments in Figures 1F and 1G and Figure 3C. H.C. carried out the experiments in Figures 3D and 3E. M.N. and J.-H.L. carried out the experiments in Figure 1H. S.L.H. and J.A.S. conceived the study and wrote the manuscript. J.A.S. oversaw and contributed to all experimental design and the writing of the manuscript. D.B.R. contributed to experimental design of Figures 1 and 6. J.B.W., L.M.B., M.C., S.M.A., H.C., and D.B.R. reviewed the manuscript.

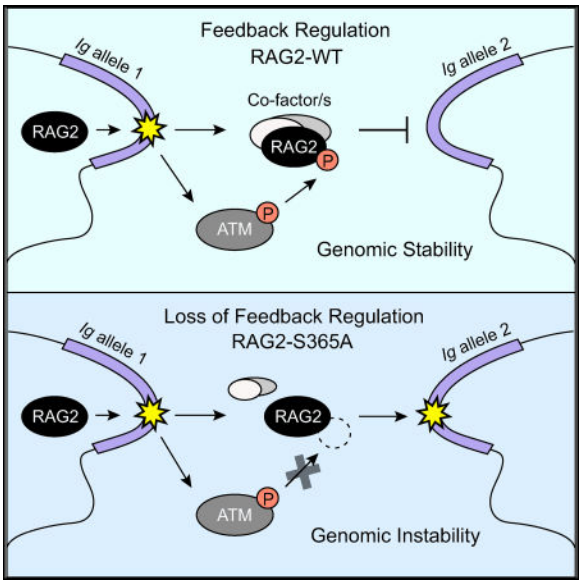

DNA lesions associated with lymphoid malignancies are linked to off-target cleavage by the RAG1/2 recombinase. Off-target RAG cleavage has only been analyzed in the context of DNA repair defects. Here, Hewitt et al. identify a phosphorylation site on RAG2 that controls RAG cleavage to maintain genome stability independent of a repair defect.

INTRODUCTION

Adaptive immunity relies on B and T cell receptor-mediated responses to foreign pathogen. A limitless universe of foreign antigens, however, requires recognition by a matched repertoire of antigen receptors, but there are only seven antigen receptor loci: three immunoglobulin (*Ig*) and four T cell receptor (*Tcr*) loci. Lymphocytes make use of this limited genetic material to generate diversity by recombining variable (V), diversity (D), and joining (J) gene segments that are arrayed along each locus (Helmink and Sleckman, 2012; Tonegawa, 1983). This process is mediated by the lymphoid-specific recombinase proteins RAG1 and RAG2 (Oettinger et al., 1990; Schatz et al., 1989) that bind at well-defined recombination signal sequences (RSSs) flanking each coding V, D, or J gene segment. RSSs consist of highly conserved heptamer and less conserved nonamer sequences that are separated by a 12- or 23-bp spacer. Although it is the RAG1 protein that specifically recognizes these sequences and catalyzes DNA cleavage at the border of the RSS and the coding gene segment (Kim et al., 1999; Landree et al., 1999), RAG2 is an equally essential accessory protein. An absence of either functional RAG1 or RAG2 abrogates V(D)J recombination (Mombaerts et al., 1992; Shinkai et al., 1992; Spanopoulou et al., 1994), resulting in severe immunodeficiency (Schwarz et al., 1996; Villa et al., 1998).

DNA cleavage by RAG1/2 results in two covalently sealed hairpins on the coding ends and two blunt signal ends. These four broken ends are held together by RAG1/2 within a stable post-cleavage complex (Agrawal and Schatz, 1997; Wang et al., 2012), which directs repair via the ubiquitous non-homologous end-joining (NHEJ) pathway and suppresses the use of other error-prone repair pathways (Lee et al., 2004). Repair of recombination intermediates

also requires the action of the DNA damage response pathway, which involves the factors ATM, γH2AX, 53BP1, and the MRN complex.

The fact that RAG2 mutations can promote lymphoid malignancies highlights a paradox of the V(D)J recombination process, namely, that the generation of diversity within antigen receptor loci entails considerable risk. DNA double-strand breaks (DSBs) are an inherent feature of recombination, and these, by their very nature, are a threat to genome stability. Furthermore, it has been estimated that cryptic RSSs are found every 1 to 2 kb within the genome and these are all potential targets for RAG. Indeed, numerous B and T acute lymphoblastic leukemias (ALLs) are associated with RAG-mediated damage occurring at cryptic RSS sites within non-antigen receptor loci, such as *IKZF1, Notch1, SIL-SCL, Bcl11b, PTEN, ETV6, BTG1, TBL1XR1*, and *CDKN2A-CDKN2B* (Mendes et al., 2014; Mullighan et al., 2008; Onozawa and Aplan, 2012; Papaemmanuil et al., 2014). Because off-targeting by RAG is known to generate translocations and changes in gene regulation as well as downstream protein production and stability that contribute to oncogenesis, it is important to understand the control mechanisms that prevent this occurring in normal cells.

Our previous studies have implicated the C terminus of RAG2 and ATM in feedback control of RAG activity (Chaumeil et al., 2013b; Hewitt et al., 2009). Specifically, we discovered that inhibition of ATM kinase activity or truncation of RAG2 leads to bi-allelic and bi-locus breaks in the same cell linked to the occurrence of translocations. However, we were not able to determine whether ATM and the C terminus of RAG2 act in the same pathway and we provided no mechanistic explanation for how cleavage is controlled. Furthermore, both ATM and the C terminus of RAG2 have numerous other functions beyond feedback control, including contributing to the stability of the RAG post-cleavage complex (Coussens et al., 2013; Deriano et al., 2011). Hence, it is not clear how much of the genome instability that occurs in their absence results from a defect in repair versus deregulated cleavage. Here, we address both issues.

Our studies describe a conserved SQ phosphorylation site on RAG2 (residues 365 to 366) that recapitulates the function of the C terminus of RAG2 and ATM in preventing bi-allelic and bi-locus cleavage in the same cell, independent of an associated repair defect. Thus, mutation of serine 365 to a non-phosphorylatable alanine provides a tool for analyzing the impact of deregulated RAG cleavage on genome instability independent of repair abnormalities. Using this RAG2 mutant, we found that an increased number of cleavage events in individual cells is linked to the occurrence of reciprocal translocations.

To further investigate control of cleavage and the connection between ATM and RAG2-S365, we asked whether a phosphomimetic of RAG2-S365 (that could potentially act as a constitutively active phosphorylated residue) might compensate for inactivation of ATM kinase activity. Indeed, the phosphomimetic RAG2-S365E rescued the cleavage defect of ATM kinase inactivation, reducing the incidence of reciprocal translocations. Together, these data strongly suggest that ATM-mediated phosphorylation of RAG2-S365 is important for feedback control of RAG cleavage and the maintenance of genome stability. Furthermore, mutated RAG2-S365 provides a setting to investigate the impact of DNA DSBs on

endogenous translocations in the absence of either the artificial introduction of breaks or a defect in repair.

RESULTS

The RAG2 Residue at Serine 365 Prevents Bi-allelic Cleavage of *Igk*

To investigate the contribution of RAG2 in controlling rearrangement on individual alleles in recombining B cells, we focused on the regulation of the immunoglobulin light chain locus, *Igk*. Rearrangement of *Igk* occurs during the small pre-B cell stage of development (Figure 1A), and in mice, it is predominantly the products of rearranged *Igk* loci and rearranged *Ig* heavy chain loci (*Igh*) that make up the B cell receptor (Bassing et al., 2002; Hardy et al., 1991; Schatz and Ji, 2011; ten Boekel et al., 1995). *Igk* was selected for analysis for the following reasons. First, *Igk* undergoes a single V-to-J recombination step in contrast to the two-step D-to-J and V-to-DJ rearrangement of the *Igh* locus. Second, small pre-B cells are not cycling so this alleviates potential effects of the DNA damage response activating any cell cycle check points. Finally, in our previous work, we demonstrated highly significant levels of bi-allelic cleavage on this locus in the absence of ATM (Hewitt et al., 2009).

As a starting point, we verified that an absence of the C terminus of RAG2 impacts cleavage on *Igk* in a similar manner to the *Tcra* locus using sorted pre-B cells derived from wild-type mice and mice expressing truncated RAG2 proteins ($Rag2^{352/352}$ and $Rag2^{FS361/FS361}$ mice) (Akamatsu et al., 2003; Akamatsu and Oettinger, 1998; Cuomo and Oettinger, 1994; Liang et al., 2002; Mijušković et al., 2015). Immuno-fluorescence in situ hybridization (immuno-FISH) experiments were performed to visualize *Igk* using DNA probes that hybridize to the 5′ and 3′ ends of the 3.2 Mb locus (Figure S1A, red and green signals), combined with an antibody to the phosphorylated form of histone H2AX, γH2AX (white signal) (Rogakou et al., 1998) as a readout for DNA DSBs. In these experiments, cells were categorized as having one, both, or no *Igk* alleles directly associated with a γH2AX-containing DNA repair focus (Figure S1A, top and bottom panels). It should be noted that colocalization of γH2AX foci with the *Igk* locus is strictly dependent on the recombinase proteins because foci were rarely associated with the *Igk* locus in $Rag1^{-/-}$ pre-B cells (Figure S1B). As expected, we found γH2AX predominantly colocalized with one *Igk* allele per cell in wild-type cells (Figure S1C) (Hewitt et al., 2009). In contrast, in pre-B cells expressing RAG2-352, we detected an increase in the frequency of bi-allelic *Igk* breaks (Figure S1C). This increase was highly significant and reproducible across independent experiments (Figure S1C; Table S1), verifying our previous findings with the *Tcra* locus (Chaumeil et al., 2013b). To complement the analysis of the RAG2-352 mice, we also analyzed breaks on *Igk* in pre-B cells from the RAG2-FS361 mouse, which contains a frameshift codon at position 361 that also leads to the production of a truncated protein (Gigi et al., 2014). As expected, mono-allelic versus bi-allelic cleavage was altered in a similar manner to RAG2-352-expressing cells (Figure S1D; Table S1).

Both the RAG2-352 and RAG2-FS361 mutants are associated with repair defects, and delayed resolution of breaks could feasibly account for an increase in the number of γH2AX foci found in each cell. To determine whether mutations associated with repair defects could impact the introduction of bi-allelic breaks on *Igk*, we next examined pre-B cells from mice

deficient in the DNA damage response factor 53BP1. As shown in Figure S1E and Table S1, an absence of 53BP1 led to a significant increase in mono-allelic breaks, without any impact on the frequency of bi-allelic cleavage. To determine whether a defect in cell cycle checkpoints had any impact on the level of mono-versus bi-allelic breaks, we also examined $p53^{-/-}$ pre-B cells, but found no difference compared to wild-type (Figure S1F; Table S1). Taken together, our data indicate that RAG2 may act to prevent simultaneous recombination on two *Igk* alleles within the same cell through mechanisms independent of repair and cell cycle checkpoints.

Several defects are known to be associated with truncated RAG2 proteins, and it remains unclear which functional domains contribute to each effect (Akamatsu and Oettinger, 1998; Corneo et al., 2007; Curry and Schlissel, 2008; Deriano et al., 2011; Kirch et al., 1998; Liang et al., 2002; Sekiguchi et al., 2001; Talukder et al., 2004) (Figure 1B). To counter these complex phenotypes, we undertook a systematic protein motif analysis to determine which properties of RAG2 might impact the control of mono-allelic versus bi-allelic cleavage of the *Igk* locus. Given our previous results, we reasoned that ATM and RAG2 could act in the same pathway and one potential level of control could be via ATM-mediated phosphorylation of RAG2.

To investigate, we focused on potential phosphorylation targets that could lie downstream of the DNA damage response. The family of phosphatidylinositol-3 kinase-related kinases (PIKKs) includes both ATM and DNA-PKcs, which are involved in the repair of RAG-mediated cleavage during V(D)J recombination (Lempiäinen and Halazonetis, 2009; Lovejoy and Cortez, 2009). The PIKKs preferentially phosphorylate their substrates on serine or threonine residues that precede glutamine residues, commonly known as SQ/TQ motifs, and there are three within the RAG2 protein (Figure 1B). The first at residues T165/Q166 is only conserved between mouse (*M. musculus*) and rat (*R. norvegicus*) (MAFFT version 7) (Katoh and Standley, 2013) (Figure 1C). The second PIKK motif at residues T264/Q265 is conserved between humans (*H. sapiens*) and mice, but not coelacanths (*L. chalumnae*) and zebrafish (*D. rerio*). In contrast, the third potential PIKK target, the S365/Q366 motif, is conserved across multiple species, including humans, mice, rats, coelacanths, zebrafish, and elephant sharks (*C. milii*) (MAFFT version 7) (Katoh and Standley, 2013), and as previously shown (Fugmann and Schatz, 2001; Lin et al., 1999).

To examine the contribution of each SQ and TQ motif to allelic control of RAG-mediated cleavage, we mutated them separately to non-phosphorylatable AQ motifs and introduced them into $Rag2^{-/-}$ (v)-Abl kinase-transformed pro-B cells lines by retroviral infection (Bredemeyer et al., 2008; Schlissel et al., 1991) (Figure 1D). Cells were subsequently treated with the v-Abl inhibitor STI571 for 40 hr to induce G1-phase cell cycle arrest and RAG upregulation for V(D)J recombination (Bredemeyer et al., 2006; Muljo and Schlissel, 2003). FISH experiments were performed to visualize the *Igk* locus, combined with a γH2AX antibody as a readout for DSBs (Figure 1E).

We first analyzed the impact of mutating serine 365 on regulation of cleavage. As shown in Figure 1F and Table S2, the RAG2-S365A mutation significantly increased bi-allelic γH2AX colocalization with *Igk*, recapitulating the effects we observed in cells expressing

the *Rag2*$^{352/352}$ protein (Figure S1C) and cells expressing wild-type RAG2 treated with an ATM kinase inhibitor (ATMi) KU-55933 (Hickson et al., 2004) (Figure 1G; Table S2). In contrast, immuno-FISH analyses of threonine to alanine mutations of the less conserved 165/166 and 264/265 TQ sites did not lead to bi-allelic colocalization of γH2AX with *Igk* (Figure S2B; Table S2). As expected, γH2AX colocalization was low in empty vector expressing control cells (Figure S2A; Table S2).

To confirm the specificity of the effect of the RAG2-S365A mutation, we additionally examined mono-allelic versus bi-allelic cleavage in *Rag2*$^{-/-}$ (v)-Abl cells expressing a construct, in which the acidic hinge region of RAG2 (where residue S365 is located) was neutralized (Neut-RAG2). A reduction of the negative charge in this domain has been linked to a repair defect and use of the alternative end-joining pathway, whereas a scrambled sequence of the hinge construct does not exhibit either of these phenotypes (Coussens et al., 2013). However, we did not detect any significant change in the frequency with which bi-allelic breaks are introduced on *Igk* in cells expressing the Neut-RAG2 mutant constructs compared to wild-type RAG2 (Figure S2C). These data further underline our findings from analyzing breaks in 53BP1-deficient cells (Figure S1E), showing that a repair defect per se is not linked to an increase in bi-allelicRAGcleavage. As an additional control, we also analyzed cleavage on *Igk* in cells expressing a RAG2 construct with a deleted PHD domain. This domain, which is found within the C-terminal region of RAG2, has been shown to be important for binding of RAG2 to the active histone modification H3K4me3 (Matthews et al., 2007). Again, we found no significant increase in bi-allelic cleavage associated with this mutation (Figure S2C). Collectively, these data suggest that the S365 residue of RAG2 has a specific role in controlling RAG-mediated cleavage so that breaks on both *Igk* alleles are not introduced simultaneously within the same cell.

Finally, to demonstrate that ATM can phosphorylate the S365 site on RAG2, we used peptides that encompass either the wild-type S365 amino acid or its mutant S365A. These were purified as glutathione S-transferase (GST) fusions and phosphorylated *in vitro* using purified ATM kinase. Phosphorylation was detected using a phospho-(ser/thr) ATM/ATR substrate antibody. As shown in Figure 1H, the wild-type peptide showed significantly more phosphorylation than the mutated peptide.

RAG2 Serine 365 Prevents Simultaneous Bi-locus Recombination of *Igk* and *Igl*

At the pre-B cell stage of B cell development, two *Ig* light chain loci, *Igk* and *Igl*, are accessible for recombination; however, *Igk* is normally recombined prior to *Igl* (Figure 1A). Our results showing that the RAG2-S365A mutant contributes to the regulation of mono-allelic RAG cleavage raises an important question. Namely, does wild-type RAG2-S365 prevent simultaneous cleavage on different loci in the same cell? In order to investigate this, we examined the level of γH2AX association on *Igl* in *Rag2*$^{-/-}$ v-Abl-transformed cell lines that were transduced with wild-type and RAG2-S365A expression constructs (as described in Figure 1D). As expected, we found only low levels of γH2AX colocalization with *Igl* in cells expressing wild-type RAG2, suggesting low levels of V(D)J recombination at this locus. In contrast, the RAG2-S365A mutant promoted significantly increased levels of γH2AX colocalization with *Igl* (Figure 2A; Table S3). Moreover, when we examined breaks

on both *Igk* and *Igl* in the same cell, we found that the increase in γH2AX association on *Igl* largely coincided with cells harboring breaks on *Igk* (Figure 2B). The increase in γH2AX association with *Igl* is comparable to the increase in bi-allelic breaks on *Igk* (Figure 2C). Examples of cells with either γH2AX colocalization on just *Igk* or both *Igk* and *Igl* alleles are shown in Figure 2D. These data point to a role for RAG2, and the S365 residue in particular, in suppressing V(D)J recombination on more than one locus at the same time in individual cells. This tight regulation of V(D)J recombination could provide a mechanism for preventing inter-locus rearrangement and for preventing the introduction of multiple DNA DSBs in the same cell, which could otherwise constitute a threat to genome stability.

Differences in RAG2-S365A Cleavage Do Not Arise from Differences in Expression, Cleavage Efficiency, Recombination, or a Defect in Repair

It is conceivable that the increase in bi-allelic, bi-locus cleavage that we detect in the RAG2-S365A cells could result from an increased level of mutant RAG2 protein. To investigate this possibility, we performed a western blot to compare protein levels in cycling and non-cycling (STI571 treated) cells expressing HA-tagged wild-type and mutant RAG2-S365A constructs. As an additional control, we also analyzed cells expressing mutant RAG2-T490A. The threonine 490 (T490) residue, located in the C-terminal region of RAG2, is phosphorylated by Cdk2 upon entry into the S phase of the cell cycle, causing RAG2 protein degradation (Li et al., 1996; Lin and Desiderio, 1993; Zhang et al., 2011). This phosphorylation event negatively regulates recombinase activity across the cell cycle, preventing RAG-mediated cleavage outside of G1. Using antibodies against the HA tags, we could only detect the non-degradable mutant RAG2-T490A protein in the untreated cycling cells (Figure 3A). In contrast, all three constructs gave rise to similar levels of RAG2 protein in the STI571-treated cells.

We also analyzed expression by immunofluorescence in individual cells. The tagged proteins reveal similar enrichment of RAG2 in euchromatic regions of the nucleus in cells expressing wild-type versus mutant RAG2-S365A constructs (Figure 3B). Furthermore, cleavage efficiency of the mutant RAG2-S365A protein was similar to wild-type RAG2, as judged by use of a pMX-INV-integrated substrate that generates GFP as a readout for recombination (Liang et al., 2002) in *Rag2*$^{-/-}$ v-Abl-transformed cells (Figure 3C). Consistent with these findings, we also detected similar levels of *Igk* recombination in cells expressing wild-type and mutant RAG2-S365A by qPCR with a Jk1 primer and a degenerate Vk primer (Figure 3D). Comparable results were obtained with semiquantitative PCR using a Vk to Jk5 primer in untreated and STI-treated cells. Here, we also analyzed recombination in cells expressing mutant T490A RAG2. Only low levels of *Igk* recombination were detected in the untreated cycling cells expressing wild-type and mutant RAG2-S365A constructs, whereas recombination occurred at slightly higher levels in the cells expressing the non-degradable RAG2-T490A construct (Figure 3E). In contrast, after STI571 treatment, we could detect no differences in the level of *Igk* recombination in cells expressing wild-type versus mutant S365A or T490A RAG2. It should be noted that even though cells expressing the non-degradable T490A mutation have an increased level of protein in untreated cycling cells, this does not lead to bi-allelic *Igk* breaks (Figure S3; Table S4). Together, these data indicate that deregulated bi-allelic, bi-locus cleavage found in cells

expressing S365A-RAG2 cannot be attributed to changes in protein levels or recombination efficiency.

ATM deficiency and an absence of the C terminus of RAG2 lead to an unstable post-cleavage complex and an increase in the alternative end-joining pathway, which contributes to the genomic instability found in lymphocytes from these mice (Barlow et al., 1996; Bredemeyer et al., 2006; Deriano et al., 2011). To determine whether RAG2-S365A gives rise to a similar defect, we used a recombination substrate to measure signal and coding joint formation (which usually occurs by classical NHEJ), including, as a negative control, the catalytically inactive RAG1 DDE mutant (Corneo et al., 2007; Kim et al., 1999; Landree et al., 1999). This assay showed normal levels of coding and signal joints in the RAG2-S365A expressing cells (Figure 3F).

To supplement these investigations, we used a substrate that can reveal repair by the error-prone alternative end-joining pathway. Expression of GFP in this assay occurs only when deletions are introduced, leading to repair that involves sequence homology within the substrate (Corneo et al., 2007). As expected, coreRAG2 (RAG2 1–383) expressing cells gave rise to alternative end-joining, but there was no evidence for use of this error-prone repair pathway in the mutant RAG2-S365A expressing cells (Figure 3G). This outcome is consistent with similar analyses performed by the Sleckman and Bassing laboratories who found that RAG2-triple TQ/SQ mutant expressing cells did not have defects in forming either signal or coding joints (Gapud et al., 2011). Together, these experiments reveal that, in contrast to ATM deficiency or an absence of the C terminus of RAG2 (coreRAG2 1–383, RAG2-352, or RAG2-FS361), mutant RAG2-S365A deregulates cleavage independent of a defect in DNA repair. These data are consistent with previous findings showing that the RAG2-S365A is dispensable for the joining step of V(D)J recombination (Gapud et al., 2011).

RAG2-S365 Contributes to Preserving Genomic Stability during V(D)J Recombination

Our data indicate that feedback control of RAG activity enforces temporally regulated cleavage so that breaks are introduced on only one allele and one locus at a time in each cell. In this respect, the RAG2-S356A mutant phenotype mirrors the phenotype of either absence of the C terminus of RAG2 or ATM deficiency, and cleavage is deregulated in all three instances. An absence of ATM or the C terminus of RAG2 is additionally known to be associated with genomic instability and the occurrence of translocations (Barlow et al., 1996; Deriano et al., 2011; Liyanage et al., 2000). However, because both these deficiencies have accompanying repair defects, it is not clear to what extent the ensuing genome instability results from deregulated cleavage versus deregulated repair.

RAG2-S365 expression provides us with a tool to study deregulated RAG cleavage and its impact on genome instability independent of any DNA repair anomaly. To investigate, we examined the stability of the *Igk* locus by metaphase spread analyses (Hewitt et al., 2004; Theunissen and Petrini, 2006). For this, we utilized the $Rag2^{-/-}$ cell lines with mutant RAG2 constructs. After allowing V(D)J recombination to occur with STI571, we prepared metaphase spreads. To evaluate damage (in the form of deletions, amplifications, and translocations), we performed DNA FISH using probes located outside of the 5′ and 3′

ends of *Igk* in combination with a paint for chromosome 6, the chromosome on which this locus is found (Figure 4A). As expected, in cells expressing control empty vector or wild-type RAG2, we detected a very low frequency of chromosomal abnormalities (Figures 4B and 4C; Table S5). In contrast, cells expressing the RAG2-S365A mutant displayed a significant increase in damage compared to wild-type RAG2 expressing cells. Interestingly, the majority of these abnormalities were reciprocal chromosomal translocations of the type shown in Figure 4A and detailed in Figure 4C. These abnormalities are qualitatively different from the types of chromosomal aberrations seen with ATM deficiency/inhibition, coreRAG2 (1–383) and Neut-RAG2, versus RAG2-S365A. In ATM deficiency/inhibition or with the coreRAG2 and Neut-RAG2 proteins, many dicentric and acentric chromosomes are detected (Coussens et al., 2013; Deriano et al., 2011). In contrast, we only rarely see this type of damage with the mutant RAG2-S365A and instead predominantly find reciprocal translocations of the type shown in Figure 4A (Figure 4C). We detect dicentric chromosomal translocations only when ATM inhibitor (ATMi) is added to RAG2-S365A (Figure 4D). These differences highlight the fact that the type of chromosomal aberrations that result from impaired negative feedback control are distinct from those arising from a repair defect.

In sum, our data suggest that the introduction of additional RAG-mediated breaks in individual cells provides additional substrates for translocations. Furthermore, for inter-locus rather than intra-locus rearrangements to occur, breaks would have to be introduced in close temporal succession and the two loci would have to be spatially proximal for *trans* locus joining.

Igk Translocates Predominantly with Chromosomes 14 and 11

Because the predominant *Igk* chromosomal abnormality associated with RAG2-S365A was reciprocal translocations, we next performed a multicolor FISH (mFISH) analysis to determine whether *Igk* translocated to the same or different partners as a result of expressing mutant RAG2 protein. This approach involves chromosome painting and allows the identification of individual chromosomes through signature staining patterns (Figure 5A). As can be seen from the analysis in Figure 5B, RAG2-S365A promotes recurrent translocations between chromosome 6 (staining pattern of green, far red, and aqua) and 11 (staining pattern of green, orange, and far red) as well as 6 and 14 (staining pattern of aqua). Other chromosomes are also translocated with chromosome 6 but at a lower frequency. Because the *Tcra/d* locus is on chromosome 14, it is possible that the translocations we detect with this chromosome involves this antigen receptor locus. However, chromosome 11 and other chromosomes identified as being involved in these reciprocal translocations do not harbor any antigen receptor loci; thus, breaks are also introduced at off-target loci.

The Phosphomimetic RAG2-S365E Can Reduce the Impact of ATM Inhibition

Together, our current and previous analyses indicate that RAG2 and the kinase activity of ATM could act in the same pathway to exert feedback control of RAG cleavage. To further investigate control of cleavage and the connection between these two factors, we asked whether phosphomimetics of serine at position 365 in RAG2 (that potentially act as constitutively phosphorylated residues) could compensate to any extent for inactivation of ATM kinase activity. Although phosphomimetics could not fix the repair defect of ATM

kinase inhibition, it is possible that they could inhibit the introduction of bi-allelic breaks on *Igk* and breaks on other loci such as *Igl*, thereby reducing the incidence of reciprocal translocations. To test this, we generated two phosphomimetics, in which the S365 residue was mutated to either aspartic acid or glutamic acid (S365D and S365E, respectively). Although the charge on both S365D and S365E is the same, the structure of the phosphomimetic S365E more closely resembles that of phosphoserine (Figure 6A). As initial controls, we verified that the S365D and S365E mutants of RAG2 were able to carry out mono-allelic cleavage of *Igk* under normal conditions and did not induce significant bi-allelic cleavage of *Igk* or cleavage of *Igl* on their own (Figures S4A–S4C; Table S6). Additionally, we verified protein levels of these phosphomimetic RAG2 proteins by using HA-tagged RAG2-S365D and RAG2-S365E expressed in transduced *Rag2*$^{-/-}$ cell lines. As seen in Figure S4D, levels of these two mutant RAG2 proteins were similar to wild-type RAG2. Further, we verified that the RAG2 phosphomimetic mutants are able to carry out signal and coding joint formation at equivalent levels to wild-type RAG2 using recombination substrates (Figure S4E).

When we examined cleavage on *Igk* in the presence of the ATMi, we found that neither of these phosphomimetics had any impact on mono-allelic *Igk* cleavage (Figure 6B). However, the phosphomimetic S365E, but not S365D, could alleviate the effects of ATM kinase inhibition by inhibiting the introduction of bi-allelic *Igk* breaks (Figure 6C; Table S6). Thus, the phosphomimetic S365E appears to be effective in combating the effect of ATM inactivation on deregulated cleavage. The fact that mono-allelic *Igk* cleavage occurred normally in the presence of S365E implies that ATM-mediated phosphorylation of residue S365 is not sufficient on its own to inhibit RAG cleavage activity and that this likely requires the co-operation of additional factors recruited downstream of the first break to prevent further cleavage from occurring.

To further validate the efficacy of this phosphomimetic, we next asked whether RAG2-S365E could reduce ATMi-mediated breaks on *Igl*. Again, we found that S365E, but not S365D, reduced the impact of ATMi treatment, limiting breaks that would otherwise be detected on *Igl* (Figure 6D; Table S6). As a final test, we asked whether a RAG2-S365E-mediated reduction in ATMi-induced deregulated cleavage could decrease the occurrence of reciprocal translocations. As can be seen in Figures 7A–7C and Table S7, the incidence of ATMi-induced reciprocal translocations was significantly reduced in cells expressing RAG2-S365E compared to RAG2-S365A and RAG2-S365D and was below that seen in wild-type RAG2-expressing cells.

Taken together, these analyses indicate that the phosphomimetic RAG2-S365E can effectively reduce the impact of ATMi treatment on feedback control of RAG cleavage and the occurrence of reciprocal translocations. These data strongly suggest that ATM-mediated phosphorylation of RAG2-S365 is important for feedback control of RAG cleavage and the maintenance of genome stability. We propose that cleavage on one allele induces phosphorylation of S365 by ATM-dependent signals, which, in co-operation with other factors, act as a feedback mechanism to prevent further breaks from being introduced until repair on the first allele is completed (Figure 8).

DISCUSSION

V(D)J recombination is tightly regulated at multiple levels in order to limit the possible hazards associated with the introduction of DSBs. Cell cycle regulated degradation of RAG2 protein (Lee and Desiderio, 1999) and control of *Rag1* expression across the cell cycle (Johnson et al., 2012) contribute; however, these mechanisms do not deal with the issue of how RAG activity is regulated in individual cells. It is critical to have such mechanisms in place to ensure that cleavage does not continue in *cis* or *trans* on accessible target loci that undergo recombination at the same stages of development as well as on actively transcribed off-target loci with cryptic RSS sites that can bind RAG (Ji et al., 2010). One potential level at which this could be controlled is regulation of *Rag* expression in response to the introduction of DSBs. Indeed, recent studies have shown that *Rag* is downregulated downstream of ATM activation (Steinel et al., 2013). Although reduced transcription undoubtedly contributes, it does not deal with the issue of how the activity of the existing RAG protein in the cell is curtailed in an immediate manner. Here, we provide strong evidence to support a model, in which ATM-mediated phosphorylation of RAG2-S365 occurs downstream of the initial V(D)J recombination event to restrain RAG activity and specifically prevent the introduction of further breaks on other alleles and loci until repair of the first cleavage event has occurred.

Our analyses lead us to conclude that mutation of RAG2-S365A results in deregulated cleavage independent of any repair defect. A number of studies have linked defective RAG targeting with leukemia, but the basis of this off-targeting is not well understood. Indeed, in murine studies, most off-target RAG cleavage events have been analyzed in the context of a DNA repair defect, confounding a clean analysis of cleavage deregulation. Mutation of serine 365 to a non-phosphorylatable alanine provides a tool for analyzing the impact of deregulated RAG cleavage on genome instability independent of repair anomalies. We found that feedback control of cleavage mediated by RAG2-S365 is important for restricting the number of substrates that could be involved in translocations. The observation that additional cleavage events incurred in cells expressing mutant RAG2-S365A can lead to translocations is important because these have only been previously demonstrated in artificial settings through, for example, irradiation or the introduction of site-specific endonuclease I-SceI-induced breaks. Our findings now establish deregulated RAG cleavage itself as a driver of chromosomal instability.

In this study, we have demonstrated that a conserved SQ phosphorylation site on RAG2 (365/366) recapitulates the temporal control of allelic cleavage exerted by ATM. This motif is a consensus phosphorylation motif for the PIKK family of kinases, which includes the DNA damage response proteins ATM and DNA-PKcs. The SQ 365/366 consensus phosphorylation site described here was previously analyzed by the Roth, Schatz, Kim, and Neal laboratories. In the first study, the Roth laboratory demonstrate that phosphorylation at two sites in RAG2 (T264 and S365) was not required for coding-end hairpin opening or for joining intermediates (Lin et al., 1999). The second report examined residues in RAG2 that might be required for DNA binding by the RAG1/RAG2 complex in *in vitro* cleavage, nicking, hairpin formation, and pre-cleavage substrate/enzyme stability assays that used a 12-RSS signal substrate (Fugmann and Schatz, 2001). Neither of these reports detects

differences between wild-type and the S365A-mutated RAG2. The third report from the Kim laboratory specifically investigated the role of DNA-PK in the V(D)J recombination process (Hah et al., 2007). They conclude that this kinase can phosphorylate RAG2 at the conserved S365 residue *in vitro*, which in malignant glioblastoma cells may downregulate RAG recombinase activity on an artificial recombination substrate. The most recent study from Neal and colleagues analyzed clusters of putative phosphorylation sites within RAG2, and found that they can contribute to limiting signal end joining by ATM (Meek et al., 2016). This report provides a provocative analysis of the contribution of potential clusters of phosphorylation sites to repair during V(D)J recombination, but does not examine the preeminence of individual sites or their contribution to cleavage regulation. In sum, previous results suggest that RAG2 may indeed undergo phosphorylation *in vivo*; however, the temporal regulation of recombination and its downstream effects were not analyzed. Furthermore, PIKK proteins have substantial redundancy between family members (Burma et al., 2001; Stiff et al., 2004), and even though DNA-PK can phosphorylate RAG2, it may only do this in vitro in the absence of other PIKKs such as ATM, which we now show is also capable of phosphorylating RAG2 at position S365.

The RAG2 S365 residue has additionally been investigated by the Sleckman laboratory in the context of a triple mutation of all three TQ or SQ motifs within RAG2 to non-phosphorylatable AQ residues (RAG2-3AQ) (Gapud et al., 2011). Consistent with our current findings, Sleckman and colleagues observed robust rearrangement of both an integrated inversional substrate pMX-INV and similar levels of *Igk* Vk to Jk rearrangements compared to wild-type RAG2. This report concluded that the SQ or TQ consensus sites in both RAG1 and RAG2 are dispensable for the joining phase of the V(D)J recombination reaction and thus RAG2-S365 is not involved in repair. However, none of these studies examined feedback regulation of cleavage and genome stability.

Our data support a model in which feedback control of cleavage and maintenance of genome stability involves ATM-mediated phosphorylation of RAG2. However, we do not know if this effect is localized to a single recombination center where recombination is going on or is a global effect that impacts all the RAG in the nucleus. We speculate that the effect is localized because it is unlikely that RAG cleavage on a single antigen receptor allele activates the entire pool of ATM in the nucleus because the latter has a myriad of effects on other signaling pathways and activation likely occurs in a controlled manner. If ATM activation is localized, its impact on RAG2 will also be localized, controlling cleavage on closely associated RAG enriched loci, which will make detection of this event difficult. Although RAG is found throughout euchromatic regions of the nucleus (Figure 3B) and is bound genome wide to H3K4me3-enriched sites (Ji et al., 2010), we know that RAG cleavage is inherently inefficient because breaks are detected on target loci in approximately 20% or less of cells. Increasing the local concentration of RAG in recombination centers through aggregation of RAG-bound loci may be important for promoting and controlling cleavage. Our current data support this idea because (1) we know that expression of RAG proteins brings recombining homologous as well as heterologous antigen receptor alleles together in the nucleus prior to cleavage (Chaumeil et al., 2013a, 2013b; Chaumeil and Skok, 2013; Hewitt et al., 2009); (2) we have also found that RAG brings a subset of RAG-enriched genes into close contact with recombining loci (Chaumeil et al., 2013b; Chaumeil

and Skok, 2013); and (3) mutant RAG2-S365A-expressing cells generate reciprocal translocations between *Igk* and other loci. Moreover, for inter-locus rather than intra-locus rearrangements to occur, breaks would have to be introduced in close temporal succession and the two loci would have to be spatially proximal for *trans* locus joining. Further investigations using live imaging systems will need to be performed to determine if this model is correct.

The involvement of ATM in feedback control implies that deregulated cleavage and off-site targeting by RAG could be associated with defects in any damage response protein that impacts ATM activation. Indeed, patients carrying mutations in DNA repair proteins, such as ATM, NBS1, and MRE11, commonly present with lymphoid malignancies (Lavin, 2008). The immune system defects in these A-T and A-T-related disorders are primarily thought to result from the aberrant repair of RAG-mediated cleavage events. However, our data suggest that deregulated RAG cleavage and off-site targeting are also likely to contribute. Given that cryptic RSSs are found every 1 to 2 kb within the genome, understanding the factors that determine which genes are hit at each stage of B and T cell development will be the next challenge.

EXPERIMENTAL PROCEDURES

Animal care was approved by the Institutional Animal Care and Use Committee under protocol number 120315-03 (NYU School of Medicine). For further description, see Supplemental Experimental Procedures.

DNA FISH with Immunofluorescence Analyses

BAC clones RPCI-24-387E13 (*Igk* C), RPCI-23-101G13 (*Igk* V), and RPCI-23-247I11 (*Igl*) were labeled by nick translation with ChromaTide Alexa Fluor 488-5 or 594-5-dUTP (Life Technologies) or Cy3- or Cy5-dUTP (GE Healthcare). DNA FISH with immunofluorescence was imaged by confocal microscopy on a Leica SP5 AOBS system (Acousto-Optical Beam Splitter). Combined detection of γH2AX and *Igk* or *Igl* probes cells was carried out as previously described (Hewitt et al., 2009).

Retroviral infections and selections were carried out in $Rag2^{-/-}$ v-Abl-transformed B cells that additionally express a *Bcl2* transgene (Bredemeyer et al., 2008). Cells were treated with 3 μM STI571 for 40 hr for DNA FISH and immunofluorescence or 1 μM for 72 hr for metaphase spread analysis.

Statistical significances were calculated by a two-tailed Fisher's exact test using R software and p values ≤ 5.00e−2 were taken to be significant (5.00e−2 ≥ p > 1.00e−2, *significant; 1.00e−2 ≥ p > 1.00−3, **very significant; p ≤ 1.00e−3, ***highly significant). As detailed in each case in the figure legends, p values displayed in the main figures were applied to combined data from repeated independent experiments. Data for individual experiments are displayed in Tables S1–S4 and S6 to demonstrate reproducibility.

Metaphase Spread Preparation and DNA FISH

Retrovirally transduced *Rag2*$^{-/-}$ v-Abl-transformed B cells were treated with 1 μM STI571 for 72 hr, washed three times with fresh media, and re-cultured in RPMI media as described above, except 20% fetal calf serum (FCS) was used. Cells were cultured for a further 40 hr to allow re-entry into the cell cycle. Metaphase spreads were prepared, and DNA FISH was performed as previously described (Hewitt et al., 2004; Theunissen and Petrini, 2006).

BAC clones RPCI-24-218K16 (*Igk* 5′) and RPCI-24-507J1 (*Igk* 3′) were labeled by nick translation, and XCP Red XCyting Mouse Chromosome 6 paint (Texas Red; MetaSystems) was prepared separately according to the supplier's instructions.

Metaphase spreads were imaged and analyzed using a Metafer microscope and ISIS software (Metasystems).

mFISH

Metaphase chromosome spreads were prepared as described above. 21×Mouse (Metasystems) chromosome painting probes were prepared according to the supplier's instructions and metaphase spreads were imaged and analyzed using a Metafer microscope and ISIS software (Metasystems).

Supplementary Material

Refer to Web version on PubMed Central for supplementary material.

Acknowledgments

The authors would like to thank members of the Skok lab for thoughtful discussions and critical comment on the study and manuscript. v-Abl-transformed B cell lines were kindly provided by Craig Bassing and Barry Sleckman. The authors would like to thank the NYU Flow Cytometry and Cell Sorting Center, supported in part by grant 5P30CA016087-33 from the National Cancer Institute. S.L.H. was previously supported by an American Society of Hematology (ASH) Scholar Award and a Molecular Oncology and Immunology Training Grant NIH T32 CA009161 (Levy). J.B.W. is supported by a Molecular Oncology and Immunology Training Grant NIH T32 CA009161 (Levy). N.M. is supported by an NCC grant. L.M.B. is supported by a Genome Integrity Training Grant NIH T32 GM115313. J.A.S. was supported by the Leukemia & Lymphoma Society (LLS) scholar and NIH grants R01 GM086852 and NIAID R56 A1099111 and is currently supported by R35GM122515. D.B.R. is supported by NIH grant R01 CA104588.

References

Agrawal A, Schatz DG. RAG1 and RAG2 form a stable postcleavage synaptic complex with DNA containing signal ends in V(D)J recombination. Cell. 1997; 89:43–53. [PubMed: 9094713]

Akamatsu Y, Oettinger MA. Distinct roles of RAG1 and RAG2 in binding the V(D)J recombination signal sequences. Mol. Cell. Biol. 1998; 18:4670–4678. [PubMed: 9671477]

Akamatsu Y, Monroe R, Dudley DD, Elkin SK, Gartner F, Talukder SR, Takahama Y, Alt FW, Bassing CH, Oettinger MA. Deletion of the RAG2 C terminus leads to impaired lymphoid development in mice. Proc. Natl. Acad. Sci. USA. 2003; 100:1209–1214. [PubMed: 12531919]

Barlow C, Hirotsune S, Paylor R, Liyanage M, Eckhaus M, Collins F, Shiloh Y, Crawley JN, Ried T, Tagle D, et al. Atm-deficient mice: a paradigm of ataxia telangiectasia. Cell. 1996; 86:159–171. [PubMed: 8689683]

Bassing CH, Swat W, Alt FW. The mechanism and regulation of chromosomal V(D)J recombination. Cell. 2002; 109(Suppl):S45–S55. [PubMed: 11983152]

Bredemeyer AL, Sharma GG, Huang CY, Helmink BA, Walker LM, Khor KC, Nuskey B, Sullivan KE, Pandita TK, Bassing CH, et al. ATM stabilizes DNA double-strand-break complexes during V(D)J recombination. Nature. 2006; 442:466–470. [PubMed: 16799570]

Bredemeyer AL, Helmink BA, Innes CL, Calderon B, McGinnis LM, Mahowald GK, Gapud EJ, Walker LM, Collins JB, Weaver BK, et al. DNA double-strand breaks activate a multi-functional genetic program in developing lymphocytes. Nature. 2008; 456:819–823. [PubMed: 18849970]

Burma S, Chen BP, Murphy M, Kurimasa A, Chen DJ. ATM phosphorylates histone H2AX in response to DNA double-strand breaks. J. Biol. Chem. 2001; 276:42462–42467. [PubMed: 11571274]

Chaumeil J, Skok JA. A new take on v(d)j recombination: transcription driven nuclear and chromatin reorganization in rag-mediated cleavage. Front. Immunol. 2013; 4:423. [PubMed: 24367365]

Chaumeil J, Micsinai M, Ntziachristos P, Deriano L, Wang JM, Ji Y, Nora EP, Rodesch MJ, Jeddeloh JA, Aifantis I, et al. Higher-order looping and nuclear organization of Tcra facilitate targeted rag cleavage and regulated rearrangement in recombination centers. Cell Rep. 2013a; 3:359–370. [PubMed: 23416051]

Chaumeil J, Micsinai M, Ntziachristos P, Roth DB, Aifantis I, Kluger Y, Deriano L, Skok JA. The RAG2 C-terminus and ATM protect genome integrity by controlling antigen receptor gene cleavage. Nat. Commun. 2013b; 4:2231. [PubMed: 23900513]

Corneo B, Wendland RL, Deriano L, Cui X, Klein IA, Wong SY, Arnal S, Holub AJ, Weller GR, Pancake BA, et al. Rag mutations reveal robust alternative end joining. Nature. 2007; 449:483–486. [PubMed: 17898768]

Coussens MA, Wendland RL, Deriano L, Lindsay CR, Arnal SM, Roth DB. RAG2's acidic hinge restricts repair-pathway choice and promotes genomic stability. Cell Rep. 2013; 4:870–878. [PubMed: 23994475]

Cuomo CA, Oettinger MA. Analysis of regions of RAG-2 important for V(D)J recombination. Nucleic Acids Res. 1994; 22:1810–1814. [PubMed: 8208604]

Curry JD, Schlissel MS. RAG2's non-core domain contributes to the ordered regulation of V(D)J recombination. Nucleic Acids Res. 2008; 36:5750–5762. [PubMed: 18776220]

Deriano L, Chaumeil J, Coussens M, Multani A, Chou Y, Alekseyenko AV, Chang S, Skok JA, Roth DB. The RAG2 C terminus suppresses genomic instability and lymphomagenesis. Nature. 2011; 471:119–123. [PubMed: 21368836]

Fugmann SD, Schatz DG. Identification of basic residues in RAG2 critical for DNA binding by the RAG1-RAG2 complex. Mol. Cell. 2001; 8:899–910. [PubMed: 11684024]

Gapud EJ, Lee BS, Mahowald GK, Bassing CH, Sleckman BP. Repair of chromosomal RAG-mediated DNA breaks by mutant RAG proteins lacking phosphatidylinositol 3-like kinase consensus phosphorylation sites. J. Immunol. 2011; 187:1826–1834. [PubMed: 21742970]

Gigi V, Lewis S, Shestova O, Mijušković M, Deriano L, Meng W, Luning Prak ET, Roth DB. RAG2 mutants alter DSB repair pathway choice in vivo and illuminate the nature of 'alternative NHEJ'. Nucleic Acids Res. 2014; 42:6352–6364. [PubMed: 24753404]

Hah YS, Lee JH, Kim DR. DNA-dependent protein kinase mediates V(D)J recombination via RAG2 phosphorylation. J. Biochem. Mol. Biol. 2007; 40:432–438. [PubMed: 17562296]

Hardy RR, Carmack CE, Shinton SA, Kemp JD, Hayakawa K. Resolution and characterization of pro-B and pre-pro-B cell stages in normal mouse bone marrow. J. Exp. Med. 1991; 173:1213–1225. [PubMed: 1827140]

Helmink BA, Sleckman BP. The response to and repair of RAG-mediated DNA double-strand breaks. Annu. Rev. Immunol. 2012; 30:175–202. [PubMed: 22224778]

Hewitt SL, High FA, Reiner SL, Fisher AG, Merkenschlager M. Nuclear repositioning marks the selective exclusion of lineage-inappropriate transcription factor loci during T helper cell differentiation. Eur. J. Immunol. 2004; 34:3604–3613. [PubMed: 15484194]

Hewitt SL, Yin B, Ji Y, Chaumeil J, Marszalek K, Tenthorey J, Salvagiotto G, Steinel N, Ramsey LB, Ghysdael J, et al. RAG-1 and ATM coordinate monoallelic recombination and nuclear positioning of immunoglobulin loci. Nat. Immunol. 2009; 10:655–664. [PubMed: 19448632]

Hickson I, Zhao Y, Richardson CJ, Green SJ, Martin NM, Orr AI, Reaper PM, Jackson SP, Curtin NJ, Smith GC. Identification and characterization of a novel and specific inhibitor of the ataxia-telangiectasia mutated kinase ATM. Cancer Res. 2004; 64:9152–9159. [PubMed: 15604286]

Ji Y, Resch W, Corbett E, Yamane A, Casellas R, Schatz DG. The in vivo pattern of binding of RAG1 and RAG2 to antigen receptor loci. Cell. 2010; 141:419–431. [PubMed: 20398922]

Johnson K, Chaumeil J, Micsinai M, Wang JM, Ramsey LB, Baracho GV, Rickert RC, Strino F, Kluger Y, Farrar MA, et al. IL-7 functionally segregates the pro-B cell stage by regulating transcription of recombination mediators across cell cycle. J. Immunol. 2012; 188:6084–6092. [PubMed: 22581861]

Katoh K, Standley DM. MAFFT multiple sequence alignment software version 7: improvements in performance and usability. Mol. Biol. Evol. 2013; 30:772–780. [PubMed: 23329690]

Kim DR, Dai Y, Mundy CL, Yang W, Oettinger MA. Mutations of acidic residues in RAG1 define the active site of the V(D)J recombinase. Genes Dev. 1999; 13:3070–3080. [PubMed: 10601033]

Kirch SA, Rathbun GA, Oettinger MA. Dual role of RAG2 in V(D)J recombination: catalysis and regulation of ordered Ig gene assembly. EMBO J. 1998; 17:4881–4886. [PubMed: 9707447]

Landree MA, Wibbenmeyer JA, Roth DB. Mutational analysis of RAG1 and RAG2 identifies three catalytic amino acids in RAG1 critical for both cleavage steps of V(D)J recombination. Genes Dev. 1999; 13:3059–3069. [PubMed: 10601032]

Lavin MF. Ataxia-telangiectasia: from a rare disorder to a paradigm for cell signalling and cancer. Nat. Rev. Mol. Cell Biol. 2008; 9:759–769. [PubMed: 18813293]

Lee J, Desiderio S. Cyclin A/CDK2 regulates V(D)J recombination by coordinating RAG-2 accumulation and DNA repair. Immunity. 1999; 11:771–781. [PubMed: 10626899]

Lee GS, Neiditch MB, Salus SS, Roth DB. RAG proteins shepherd double-strand breaks to a specific pathway, suppressing error-prone repair, but RAG nicking initiates homologous recombination. Cell. 2004; 117:171–184. [PubMed: 15084256]

Lempiäinen H, Halazonetis TD. Emerging common themes in regulation of PIKKs and PI3Ks. EMBO J. 2009; 28:3067–3073. [PubMed: 19779456]

Li Z, Dordai DI, Lee J, Desiderio S. A conserved degradation signal regulates RAG-2 accumulation during cell division and links V(D)J recombination to the cell cycle. Immunity. 1996; 5:575–589. [PubMed: 8986717]

Liang HE, Hsu LY, Cado D, Cowell LG, Kelsoe G, Schlissel MS. The “dispensable” portion of RAG2 is necessary for efficient V-to-DJ rearrangement during B and T cell development. Immunity. 2002; 17:639–651. [PubMed: 12433370]

Lin W-C, Desiderio S. Regulation of V(D)J recombination activator protein RAG-2 by phosphorylation. Science. 1993; 260:953–959. [PubMed: 8493533]

Lin JM, Landree MA, Roth DB. V(D)J recombination catalyzed by mutant RAG proteins lacking consensus DNA-PK phosphorylation sites. Mol. Immunol. 1999; 36:1263–1269. [PubMed: 10684966]

Liyanage M, Weaver Z, Barlow C, Coleman A, Pankratz DG, Anderson S, Wynshaw-Boris A, Ried T. Abnormal rearrangement within the alpha/delta T-cell receptor locus in lymphomas from Atm-deficient mice. Blood. 2000; 96:1940–1946. [PubMed: 10961898]

Lovejoy CA, Cortez D. Common mechanisms of PIKK regulation. DNA Repair (Amst.). 2009; 8:1004–1008. [PubMed: 19464237]

Matthews AG, Kuo AJ, Ramón-Maiques S, Han S, Champagne KS, Ivanov D, Gallardo M, Carney D, Cheung P, Ciccone DN, et al. RAG2 PHD finger couples histone H3 lysine 4 trimethylation with V(D)J recombination. Nature. 2007; 450:1106–1110. [PubMed: 18033247]

Meek K, Xu Y, Bailie C, Yu K, Neal JA. The ATM kinase restrains joining of both VDJ signal and coding ends. J. Immunol. 2016; 197:3165–3174. [PubMed: 27574300]

Mendes RD, Sarmento LM, Canté-Barrett K, Zuurbier L, Buijs-Gladdines JG, Póvoa V, Smits WK, Abecasis M, Yunes JA, Sonneveld E, et al. PTEN microdeletions in T-cell acute lymphoblastic leukemia are caused by illegitimate RAG-mediated recombination events. Blood. 2014; 124:567–578. [PubMed: 24904117]

Mijušković M, Chou YF, Gigi V, Lindsay CR, Shestova O, Lewis SM, Roth DB. Off-target V(D)J recombination drives lymphomagenesis and is escalated by loss of the Rag2 C terminus. Cell Rep. 2015; 12:1842–1852. [PubMed: 26365182]

Mombaerts P, Iacomini J, Johnson RS, Herrup K, Tonegawa S, Papaioannou VE. RAG-1-deficient mice have no mature B and T lymphocytes. Cell. 1992; 68:869–877. [PubMed: 1547488]

Muljo SA, Schlissel MS. A small molecule Abl kinase inhibitor induces differentiation of Abelson virus-transformed pre-B cell lines. Nat. Immunol. 2003; 4:31–37. [PubMed: 12469118]

Mullighan CG, Miller CB, Radtke I, Phillips LA, Dalton J, Ma J, White D, Hughes TP, Le Beau MM, Pui CH, et al. BCR-ABL1 lymphoblastic leukaemia is characterized by the deletion of Ikaros. Nature. 2008; 453:110–114. [PubMed: 18408710]

Oettinger MA, Schatz DG, Gorka C, Baltimore D. RAG-1 and RAG-2, adjacent genes that synergistically activate V(D)J recombination. Science. 1990; 248:1517–1523. [PubMed: 2360047]

Onozawa M, Aplan PD. Illegitimate V(D)J recombination involving nonantigen receptor loci in lymphoid malignancy. Genes Chromosomes Cancer. 2012; 51:525–535. [PubMed: 22334400]

Papaemmanuil E, Rapado I, Li Y, Potter NE, Wedge DC, Tubio J, Alexandrov LB, Van Loo P, Cooke SL, Marshall J, et al. RAG-mediated recombination is the predominant driver of oncogenic rearrangement in ETV6-RUNX1 acute lymphoblastic leukemia. Nat. Genet. 2014; 46:116–125. [PubMed: 24413735]

Rogakou EP, Pilch DR, Orr AH, Ivanova VS, Bonner WM. DNA double-stranded breaks induce histone H2AX phosphorylation on serine 139. J. Biol. Chem. 1998; 273:5858–5868. [PubMed: 9488723]

Schatz DG, Ji Y. Recombination centres and the orchestration of V(D)J recombination. Nat. Rev. Immunol. 2011; 11:251–263. [PubMed: 21394103]

Schatz DG, Oettinger MA, Baltimore D. The V(D)J recombination activating gene, RAG-1. Cell. 1989; 59:1035–1048. [PubMed: 2598259]

Schlissel MS, Corcoran LM, Baltimore D. Virus-transformed pre-B cells show ordered activation but not inactivation of immunoglobulin gene rearrangement and transcription. J. Exp. Med. 1991; 173:711–720. [PubMed: 1900081]

Schwarz K, Gauss GH, Ludwig L, Pannicke U, Li Z, Lindner D, Friedrich W, Seger RA, Hansen-Hagge TE, Desiderio S, et al. RAG mutations in human B cell-negative SCID. Science. 1996; 274:97–99. [PubMed: 8810255]

Sekiguchi JA, Whitlow S, Alt FW. Increased accumulation of hybrid V(D)J joins in cells expressing truncated versus full-length RAGs. Mol. Cell. 2001; 8:1383–1390. [PubMed: 11779512]

Shinkai Y, Rathbun G, Lam KP, Oltz EM, Stewart V, Mendelsohn M, Charron J, Datta M, Young F, Stall AM, et al. RAG-2-deficient mice lack mature lymphocytes owing to inability to initiate V(D)J rearrangement. Cell. 1992; 68:855–867. [PubMed: 1547487]

Spanopoulou E, Roman CA, Corcoran LM, Schlissel MS, Silver DP, Nemazee D, Nussenzweig MC, Shinton SA, Hardy RR, Baltimore D. Functional immunoglobulin transgenes guide ordered B-cell differentiation in Rag-1-deficient mice. Genes Dev. 1994; 8:1030–1042. [PubMed: 7926785]

Steinel NC, Lee BS, Tubbs AT, Bednarski JJ, Schulte E, Yang-Iott KS, Schatz DG, Sleckman BP, Bassing CH. The ataxia telangiectasia mutated kinase controls Igκ allelic exclusion by inhibiting secondary Vκ-to-Jκ rearrangements. J. Exp. Med. 2013; 210:233–239. [PubMed: 23382544]

Stiff T, O'Driscoll M, Rief N, Iwabuchi K, Löbrich M, Jeggo PA. ATM and DNA-PK function redundantly to phosphorylate H2AX after exposure to ionizing radiation. Cancer Res. 2004; 64:2390–2396. [PubMed: 15059890]

Talukder SR, Dudley DD, Alt FW, Takahama Y, Akamatsu Y. Increased frequency of aberrant V(D)J recombination products in core RAG-expressing mice. Nucleic Acids Res. 2004; 32:4539–4549. [PubMed: 15328366]

ten Boekel E, Melchers F, Rolink A. The status of Ig loci rearrangements in single cells from different stages of B cell development. Int. Immunol. 1995; 7:1013–1019. [PubMed: 7577795]

Theunissen JW, Petrini JH. Methods for studying the cellular response to DNA damage: influence of the Mre11 complex on chromosome metabolism. Methods Enzymol. 2006; 409:251–284. [PubMed: 16793406]

Tonegawa S. Somatic generation of antibody diversity. Nature. 1983; 302:575–581. [PubMed: 6300689]

Villa A, Santagata S, Bozzi F, Giliani S, Frattini A, Imberti L, Gatta LB, Ochs HD, Schwarz K, Notarangelo LD, et al. Partial V(D)J recombination activity leads to Omenn syndrome. Cell. 1998; 93:885–896. [PubMed: 9630231]

Wang G, Dhar K, Swanson PC, Levitus M, Chang Y. Real-time monitoring of RAG-catalyzed DNA cleavage unveils dynamic changes in coding end association with the coding end complex. Nucleic Acids Res. 2012; 40:6082–6096. [PubMed: 22434887]

Zhang L, Reynolds TL, Shan X, Desiderio S. Coupling of V(D)J recombination to the cell cycle suppresses genomic instability and lymphoid tumorigenesis. Immunity. 2011; 34:163–174. [PubMed: 21349429]

Highlights

- A phosphorylation site on RAG2-S365 is involved in feedback control of RAG cleavage
- A RAG2-S365A mutation leads to bi-allelic and bi-locus RAG-mediated breaks
- Deregulated cleavage is a driver of chromosomal instability without a repair defect
- Cleavage control and maintenance of genome stability involves ATM's kinase activity

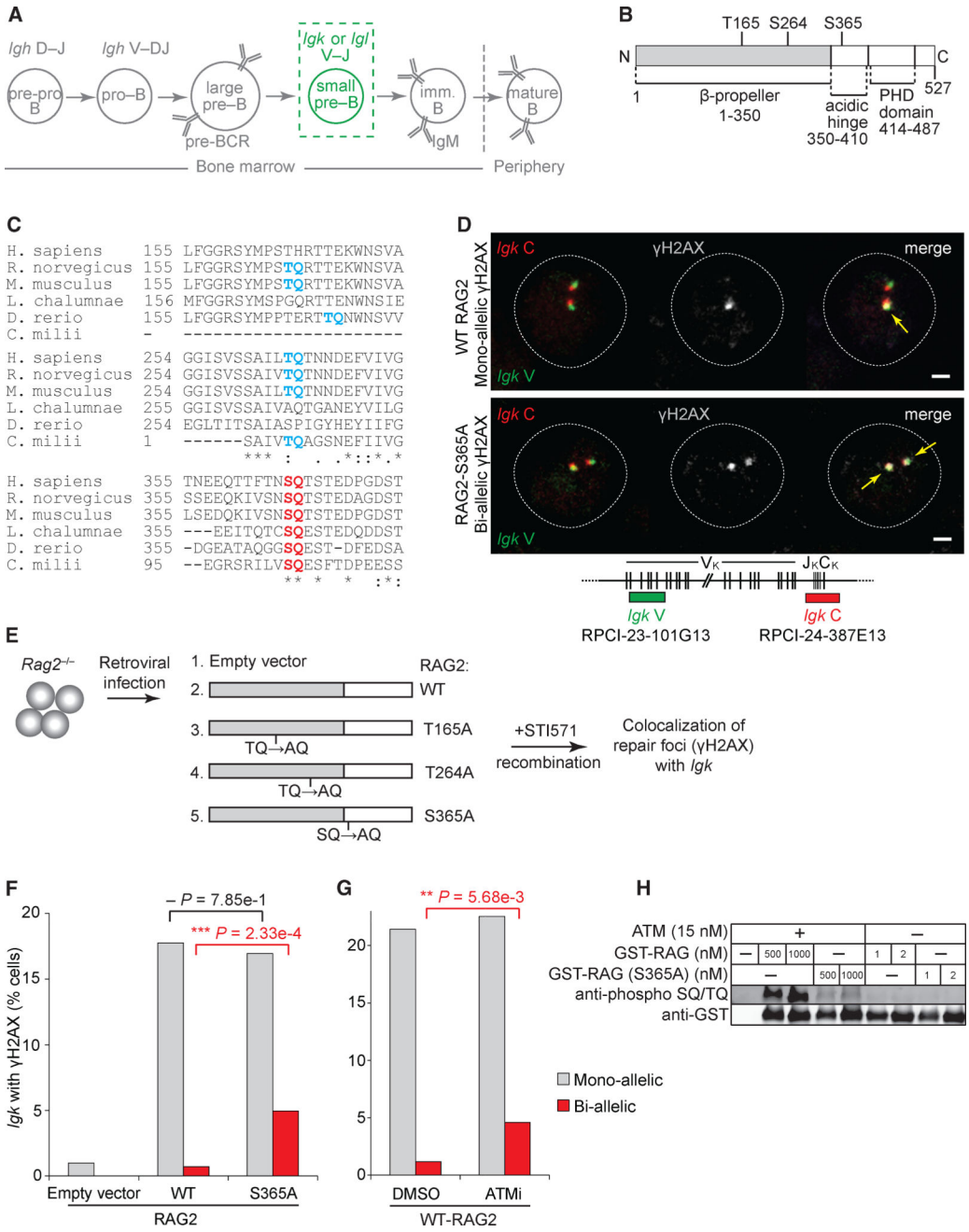

Figure 1. The Serine 365 Residue of RAG2 Is Required to Limit Cleavage to One *Igk* Allele at a Time

(A) Scheme detailing the different stages of V(D)J recombination during B cell development. Rearrangement of the *Ig* light chain loci, *Igk* or *Igl*, occurs at the pre-B cell stage.

(B) Diagram of the RAG2 protein domains, showing the β-propeller and PHD globular domains, and the intervening acidic hinge region.

(C) Conservation analysis of TQ/SQ sites in the RAG2 amino acid sequence (performed by MAFFT version 7). Numbers indicate the position of the first amino acid shown on each row within each species. Asterisks indicate conserved residues.

(D) DNA-FISH combined with immunofluorescence to detect γH2AX-containing repair foci at the *Igk* locus. The upper or lower panels show colocalization of γH2AX with one or both *Igk* alleles, respectively. Scheme depicting the position of bacterial artificial chromosome (BAC) probes used to detect both ends of the 3.2 Mb *Igk* locus is shown below. Scale bar, 1 μm.

(E) Experimental procedure for analyzing the contribution of RAG2 motifs to allelic control of *Igk* recombination. *Rag2*$^{-/-}$– v-Abl-transformed B cells were infected with retroviruses encoding an empty vector, wild-type RAG2, or individual RAG2 mutants and CD90.1, which is used as a marker of infection. Subsequent treatment of cells with the v-Abl inhibitor STI571 for 40 hr induced G1-phase cell cycle arrest, *Rag* upregulation, and V(D)J recombination.

(F and G) Colocalization of γH2AX with *Igk* in *Rag2*$^{-/-}$ v-Abl cells transduced with wild-type RAG2 versus RAG2-S365A (F) and wild-type RAG2 with DMSO versus treatment with an ATM inhibitor (G). Two independent experiments are combined for these analyses (see Table S2 for individual experiments) and *p≤5.00e−2, **p ≤ 1.00e−2, and ***p ≤ 1.00e−3 (two-tailed Fisher's exact test).

(H) RAG2 peptides that encompass either the wild-type S365 amino acid or its mutant S365A were purified as GST fusions and phosphorylated *in vitro* using purified ATM kinase. Phosphorylation was detected using a phospho-(ser/thr) ATM/ATR substrate antibody.

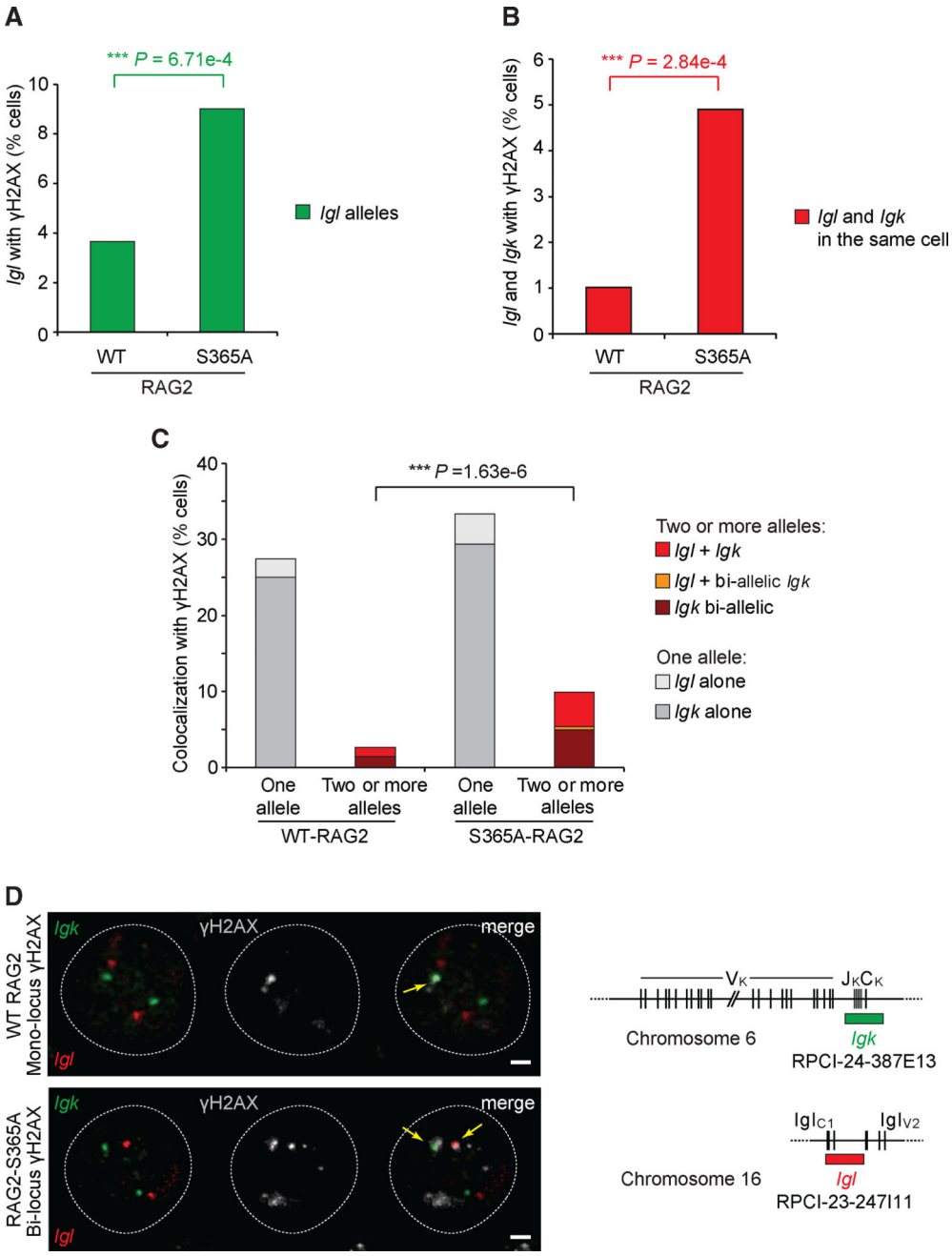

Figure 2. The RAG2 Serine 365 Residue Prevents Multiple Recombination Events on *Igk* and *Igl* Loci within Each Cell

(A) Colocalization of γH2AX-containing repair foci with *Igl* alleles in *Rag2*$^{-/-}$ v-Abl cells transduced with wild-type RAG2 or RAG2-S365A retroviruses, as in Figure 1.

(B) Colocalization of γH2AX foci with *Igl* and *Igk* loci in the same cell.

(C) Colocalization of γH2AX with either a single allele per cell (*Igl* alone or *Igk* alone) or with two or more alleles per cell (one *Igl* with one *Igk* allele or one *Igl* with two *Igk* alleles). For (A–C), two independent experiments are combined (see Table S3).

(D) Representative microscope images of γH2AX colocalization with one *Igk* allele per cell (upper panel) or simultaneously with one *Igl* and one *Igk* allele per cell (lower panel). The BAC probes used to detect the *Igl* or *Igk* loci are indicated on the right. Scale bar, 1 μm.

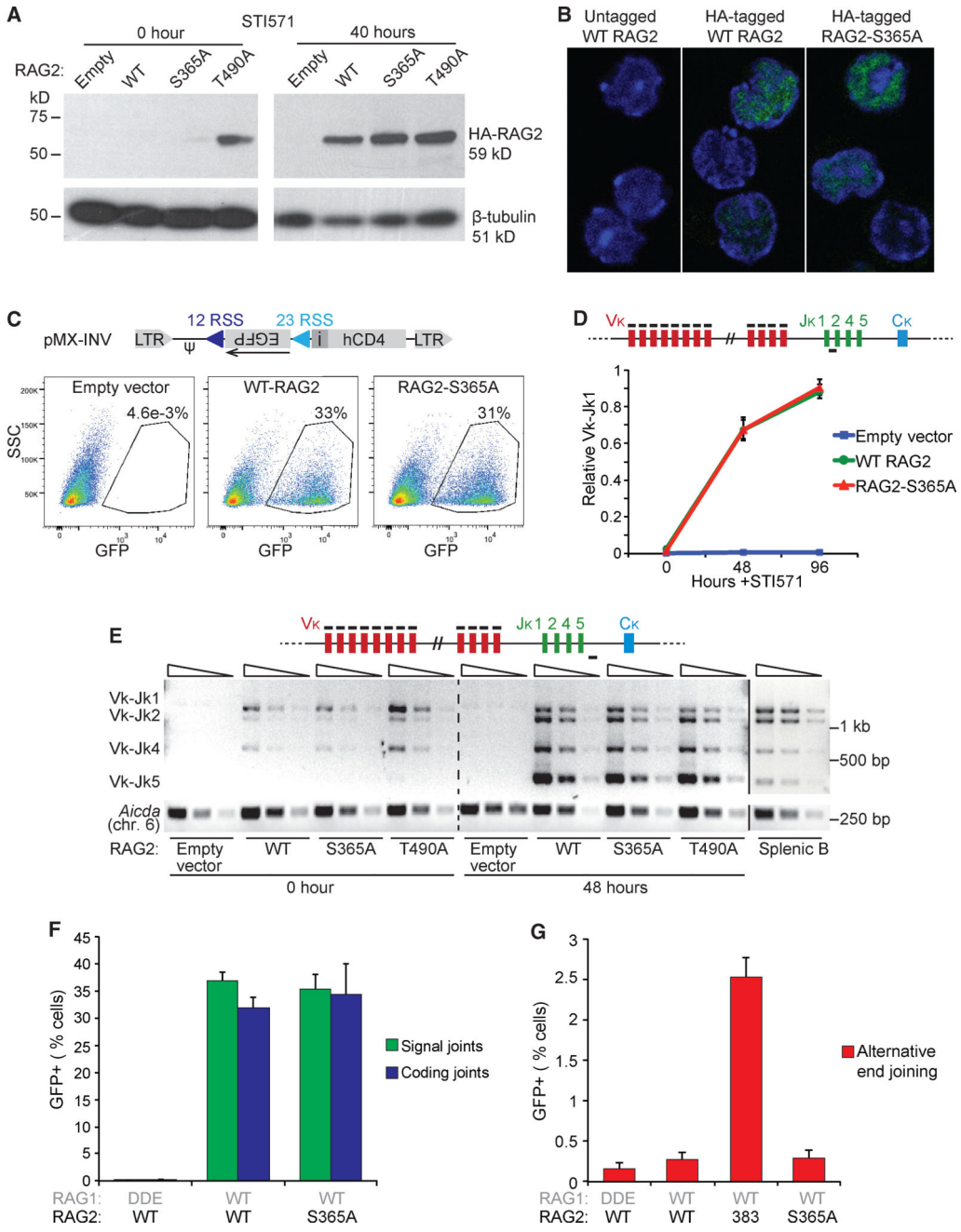

Figure 3. The RAG2-S365A Mutation Does Not Alter Recombination Efficiency or Impact Repair Pathway Choice

(A) Western blot of HA-tagged RAG2 levels shows similar levels of wild-type RAG2 or RAG2-S365A protein detected before and after STI571 treatment.

(B) Immunofluorescence of tagged RAG2 with an anti-HA antibody shows the level and distribution of wild-type and RAG2-S365A within the nucleus (blue, DAPI staining; green, HA-RAG2).

(C) Recombination efficiency of RAG2 on the chromosomal substrate pMX-INV is shown by GFP expression (scheme shown above). One copy was integrated chromosomally in *Rag2*$^{-/-}$ v-Abl cells. One of three independent experiments is shown.

(D) *Igk* recombination levels by qPCR between genomic Vk segments and Jk1 (scheme of *Igk* locus shown above, with primers in black). Experiments were carried out in triplicate and one independent experiment is shown.

(E) Semi-quantitative PCR of genomic *Igk* recombination between Vk segments and Jk1, 2, 4, and 5 in untreated and STI571-treated v-Abl cells (scheme of *Igk* locus shown above, with primers in black). Recombination levels are compared to CD19+ splenic B cells. 3-fold dilutions of input DNA are normalized to a chromosome 6 control gene (*Aicda*), and one of two independent experiments is represented.

(F) Formation of normal signal and coding joints measured with the extrachromosomal substrates pGFP-SJ pGFP-CJ (Corneo et al., 2007), which express GFP when recombination has occurred.

(G) Formation of coding joints by the alternative end-joining pathway is revealed by the extrachromosomal substrate pGFP-Alt (Corneo et al., 2007). For experiments shown in (F) and (G), 293T cells were transfected with the RAG expression vectors (as indicated) and the substrate plasmid. Experiments were carried out in triplicate; error bars represent the SD between these three triplicates and one of three independent experiments is shown.

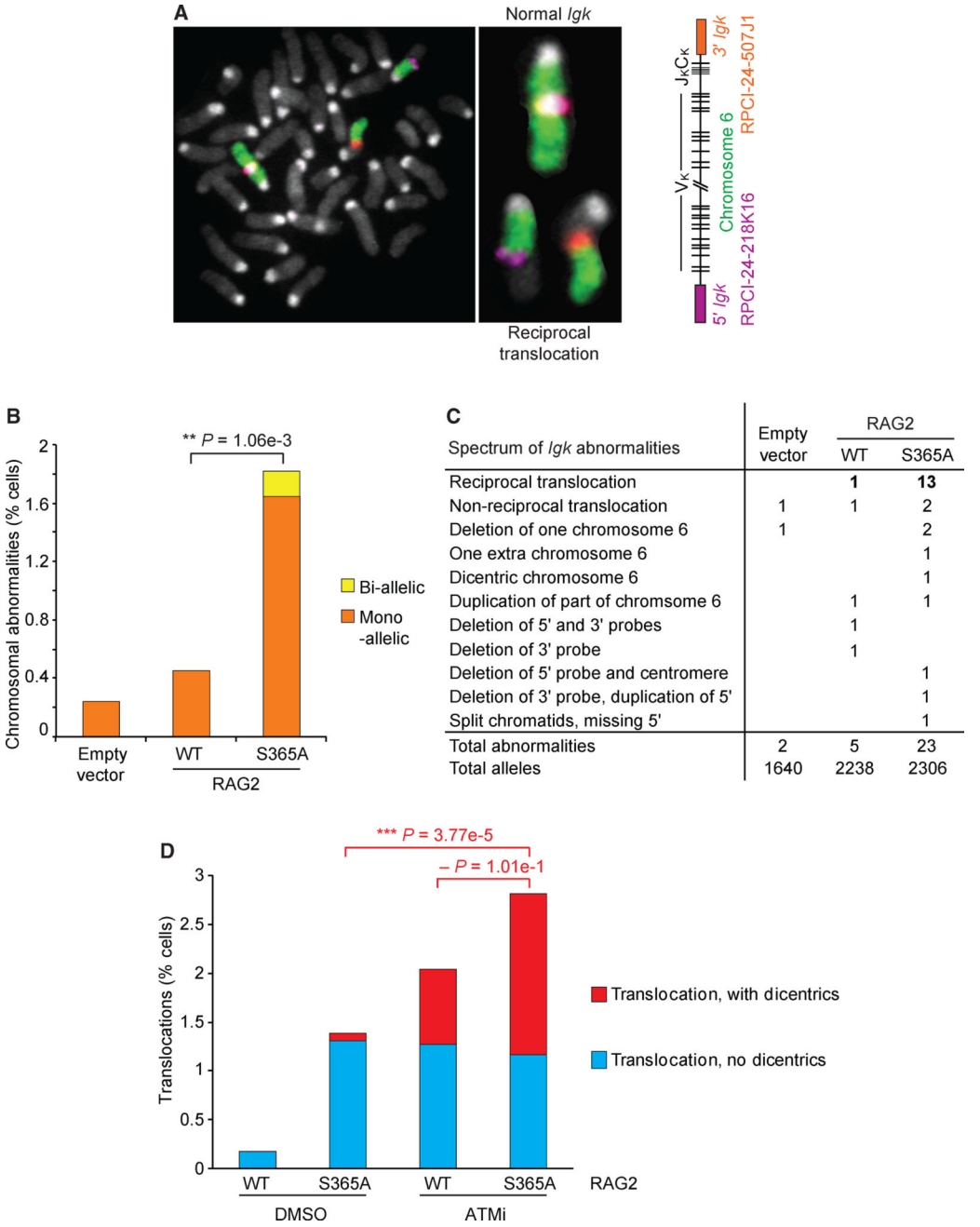

Figure 4. Mutation of RAG2-S365 Causes Instability of the *Igk* Locus

(A) Representative metaphase spread from a cell expressing RAG2-S365A (left panel), following STI571 treatment and re-entry into the cell cycle. A magnified image (right panel) shows one normal chromosome 6 containing an intact *Igk* locus and a reciprocal chromosome translocation with the *Igk* probes separated. Scheme on the right shows BAC probes positioned outside the *Igk* gene segments that were used for analysis of chromosomal instability on this locus.

(B) Percentage of cells with chromosomal abnormalities per cell in *Rag2*$^{-/-}$ v-Abl cells expressing RAG2 retroviral expression constructs, detected with the probes indicated in (A). Three independent experiments are combined (detailed in Table S5).
(C) The spectrum of chromosomal abnormalities involving the *Igk* locus listed per allele.
(D) Percentage of cells with translocations involving *Igk* that have dicentric chromosomal translocations in cells treated with control DMSO or ATMi.

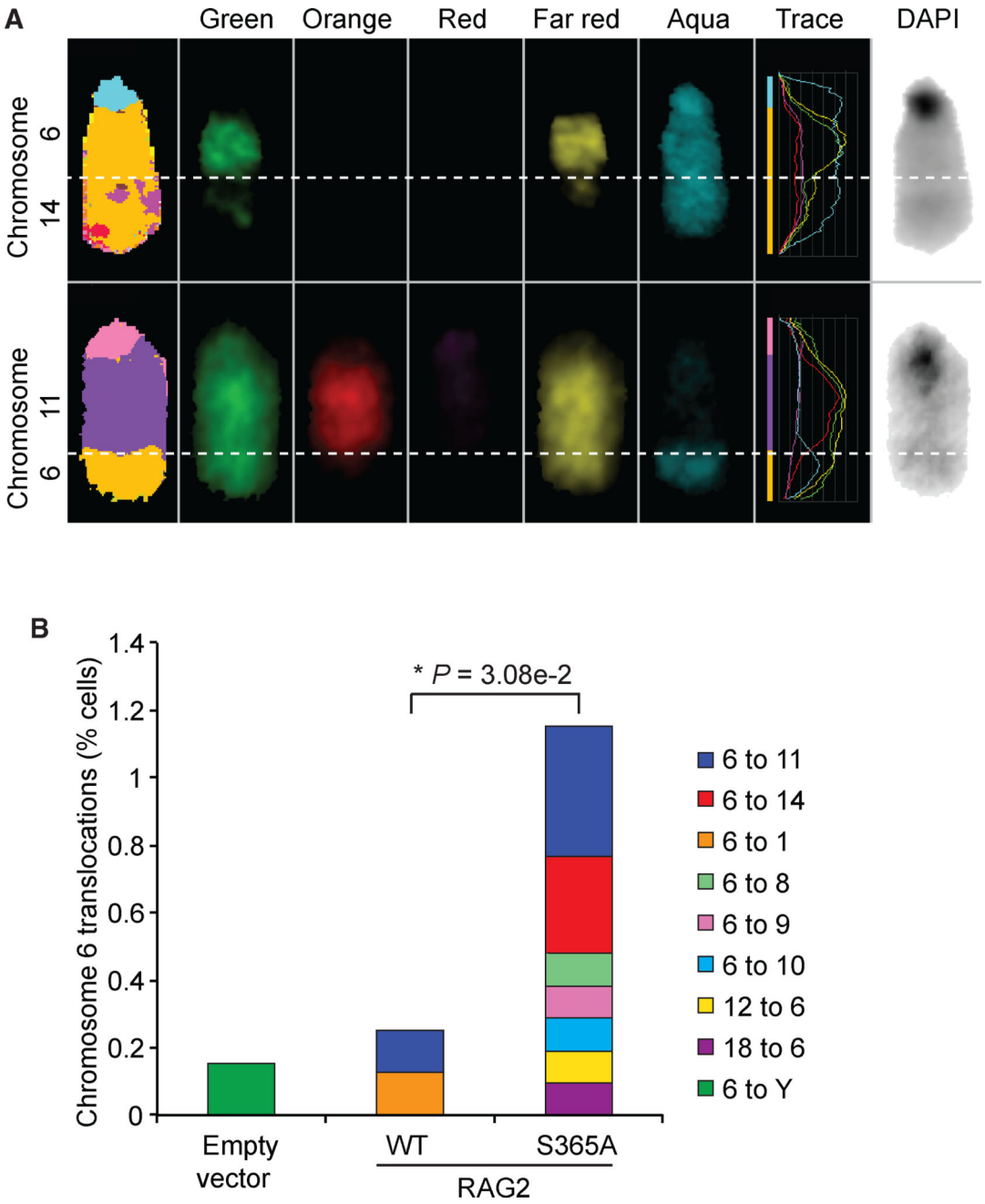

Figure 5. *Igk* Translocations Found in RAG2-S365A Expressing Cells Predominantly Partner with Chromosomes 14 and 11

(A) mFISH chromosome analysis. Two representative *Igk* translocations and their fluorescence traces.

(B) Chromosome 6 translocations are displayed as a percentage of all metaphase cells according to each partner chromosome. Two independent experiments are combined for these analyses.

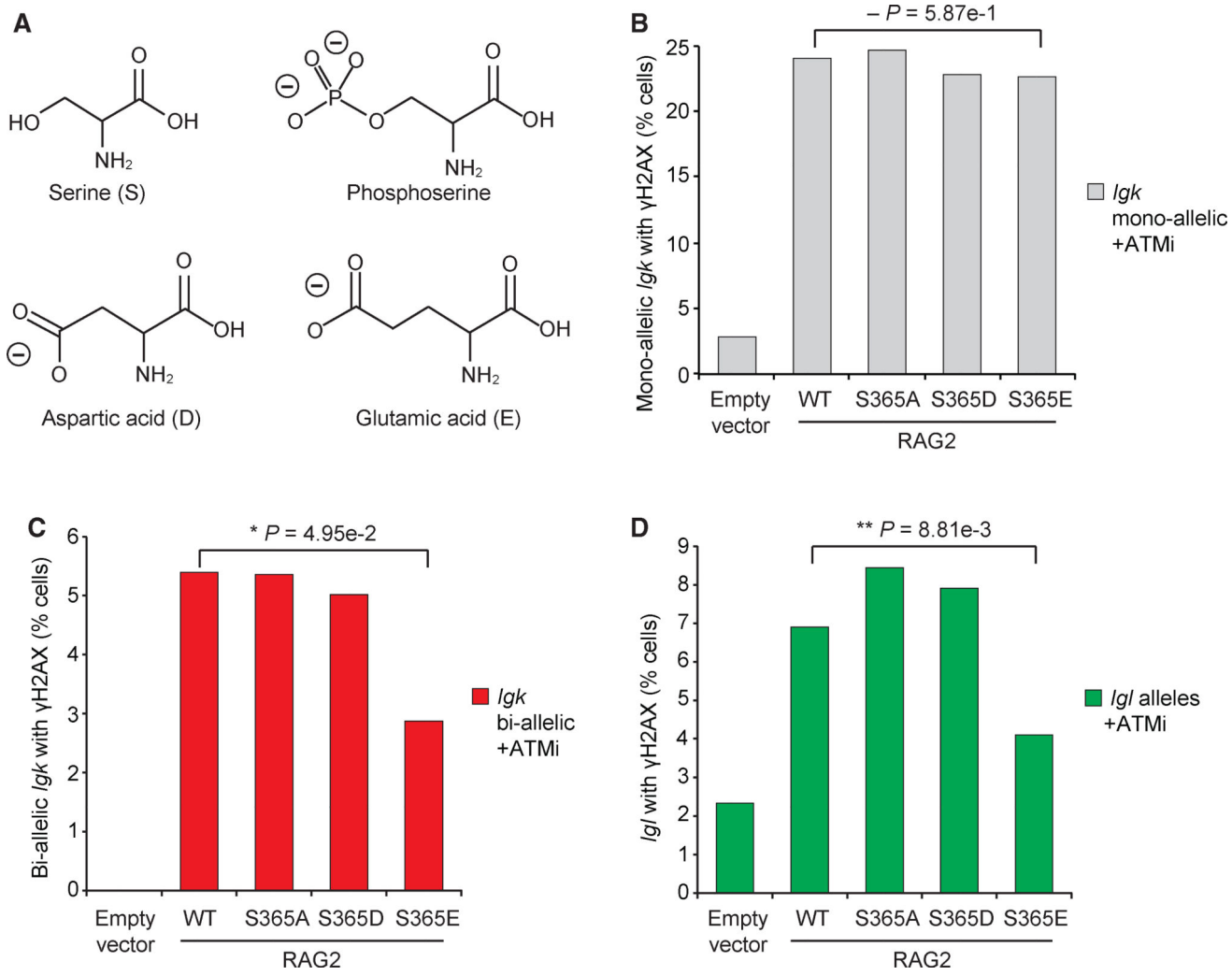

Figure 6. The Phosphomimetic Glutamic Acid at RAG2-S365 Protects against ATM-Inhibitor-Mediated Deregulated Cleavage

(A) Diagrams comparing the amino acid serine to phosphoserine and the phosphomimetics aspartic or glutamic acid.

(B–D) Colocalization of γH2AX with *Igk* or *Igl* alleles in *Rag2*$^{-/-}$ v-Abl cells transduced with RAG2 constructs and treated with both STI571 and ATMi for 40 hr; mono-allelic *Igk* (B), bi-allelic *Igk* (C), and *Igl* alleles (D). Two independent experiments are combined (see Table S6).

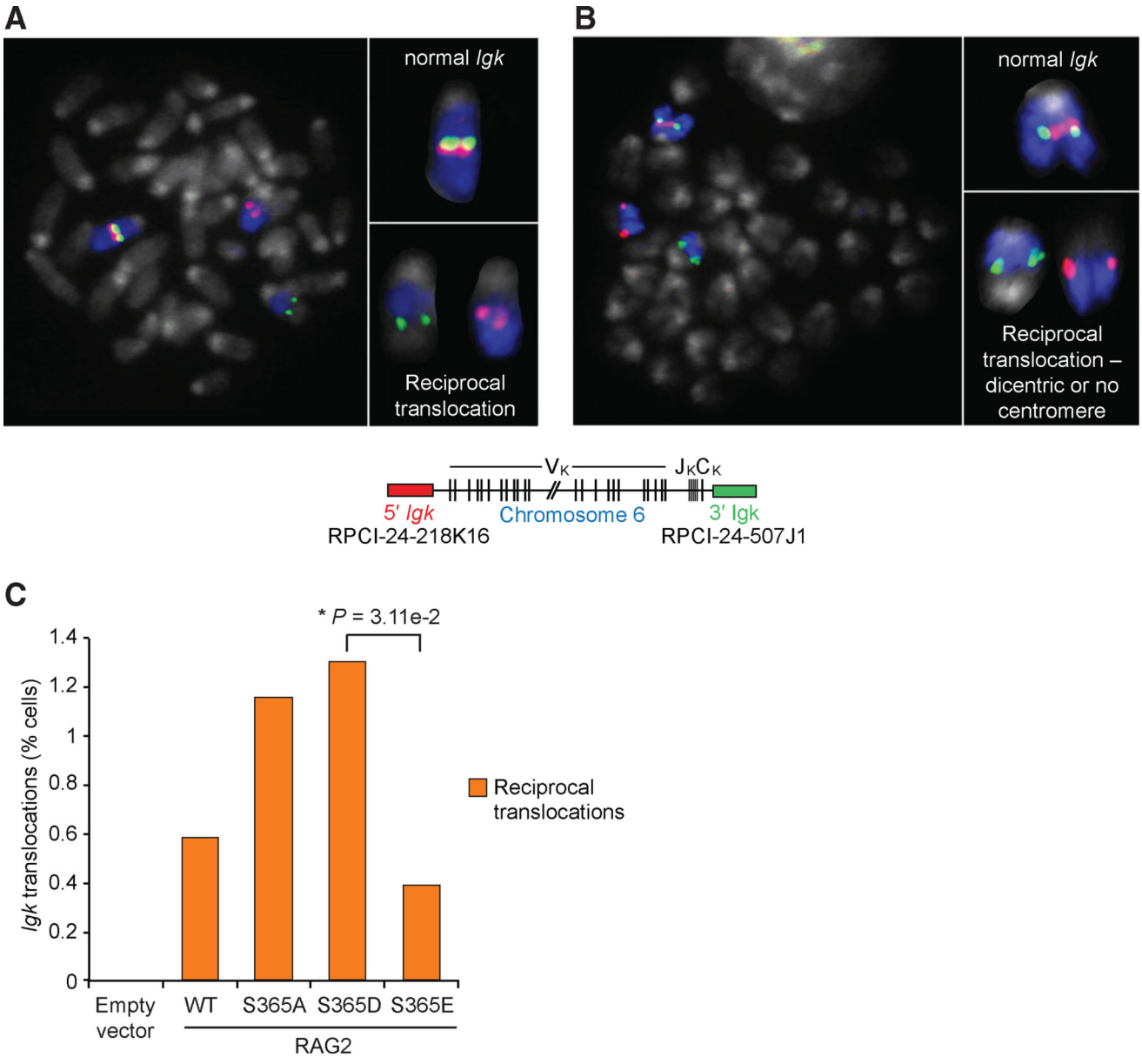

Figure 7. RAG2-S365E Protects against ATM-Inhibitor-Mediated Reciprocal Translocations

(A and B) Representative metaphase spreads, each with a reciprocal translocation. Probes used are shown in the scheme below.

(C) Percentage of reciprocal translocations detected in cells expressing different RAG2 constructs and treated with ATMi, as described in Figure 6B. Two independent experiments were combined (see Table S7).